

Temporal responses to chromatic and achromatic change inferred from temporal double-pulse integration

Keiji Uchikawa and Tatsuya Yoshizawa

Department of Intelligence Science, Tokyo Institute of Technology Graduate School, Nagatsuta, Midori-ku, Yokohama 227, Japan

Received April 21, 1992; accepted December 31, 1992; revised manuscript received January 19, 1993

Temporal integration properties of two pulses were measured for both chromatic and achromatic changes with stimulus-onset asynchronies (SOA's) of 20–2000 ms. The chromatic changes were made with respect to a reference white in both the red and the green directions by mixing 500- and 630-nm monochromatic lights at isoluminance. The achromatic changes were produced with luminance increments and decrements of the white light. In the condition of two-red (or two-green) pulse integration, a monophasic (excitatory) chromatic response was inferred, whereas in the condition of red-and-green pulse integration, a biphasic (excitatory and inhibitory) chromatic response was inferred. A biphasic achromatic response describes the results obtained in the increment-and-decrement pulse integration, and a triphasic achromatic response describes the data in two-increment (or two-decrement) pulse integration. Furthermore, it was shown that small stimulus fields of 3.4' could affect achromatic integration but not chromatic integration. We derived chromatic and achromatic impulse response functions by using a three-level color-vision model.

1. INTRODUCTION

A number of investigations have shown that, when a single pulse or a flicker stimulus is used, the temporal response to chromatic change differs from the response to achromatic change. It is generally accepted that the chromatic response has a longer integration time and low-pass-filter characteristics, whereas the achromatic response has a shorter integration time and bandpass-filter characteristics.^{1–6} These differences in temporal properties, as well as in spatial properties, between chromatic and achromatic responses are so distinct that previous investigators built models in which chromatic (opponent) and achromatic (nonopponent) channels were formed as parallel, separate mechanisms for transferring cone signals to higher levels. The assumption of this parallel model is that the chromatic channel subtracted signals from different cone types and the achromatic channel added them.^{7,8} Recently the parvocellular and the magnocellular pathways, which are found in the primate visual system, have been proposed as physiological substrates for the chromatic and the achromatic channels, respectively.^{9–11}

On the other hand, some psychophysical^{12–14} and physiological¹⁵ studies have indicated that chromatic and achromatic responses are not necessarily produced by two parallel channels but rather occur in a single mechanism according to stimulus differences in the spatiotemporal domain. Burbeck and Kelly¹² and Kelly¹³ supported this unitary model, showing that the achromatic contrast-sensitivity functions can be described as a linear subtraction of an inhibitory component from an excitatory component and that a linear addition of these excitatory and inhibitory components also could be used to explain the chromatic contrast-sensitivity function. These findings suggested that a single mechanism could form both achromatic and chromatic responses. Ingling and Martinez¹⁴ showed how the simple-opponent red-green

cell could be modeled to have both chromatic and achromatic spectral sensitivities.

It seems difficult to study an inhibitory phase following an excitatory phase of a luminance or a chromatic response in terms of critical durations measured by the single-pulse method. When flickering stimuli are used, an inhibitory phase can be inferred by using the Fourier transformation, but a prolonged repetition of flickering stimuli might cause an adaptation effect. A double-pulse method has been shown as a sensitive method for measuring a transient response.^{16–18}

In the present investigation we aim, first, to obtain integration properties of chromatic and achromatic responses by the temporal double-pulse method and, second, to derive chromatic and achromatic impulse-response functions by using an appropriate model. We used red and green isoluminant changes to measure chromatic responses and used luminance increment and decrement changes to measure achromatic responses. We also carried out experiments using small stimulus fields, to bolster our interpretation of the results.

2. METHOD

Apparatus

We used a computer-controlled six-channel Maxwellian-view system. The source was a 500-W xenon-arc lamp. Three 630-nm monochromatic lights were produced by means of monochromators with half-bandwidths of 6 nm, and three 500-nm monochromatic lights were produced by means of interference filters with half-bandwidths of 12 nm. Three pairs of 630- and 500-nm lights made test stimuli 1 and 2 and a reference white. Since all test and reference stimuli were mixtures of 500- and 630-nm monochromatic lights, isometric matches could be achieved among all these stimuli.

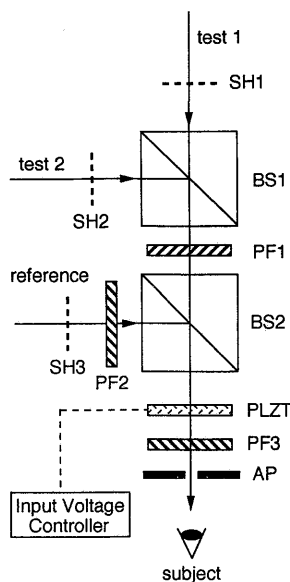


Fig. 1. Part of the apparatus that combines the three channels: test 1, test 2, and reference white. SH1, SH2, SH3, electromagnetic shutters; BS1, BS2, beam splitters; PF1, PF2, PF3, polarized filters; PLZT, lead-(Pb) lanthanum-zirconate-titanate polarizer; AP, stimulus aperture.

Six neutral-density wedges in each channel controlled luminances and chromaticities of the test and reference stimuli. As shown in Fig. 1, test stimuli 1 and 2 were combined at a beam splitter, BS1, and then the reference white was added by another beam splitter, BS2. Two polarized filters, PF1 and PF2, were placed just before BS2 in the test channels and the reference channel, respectively. Their polarizing axes were set 90 deg apart. A lead-(Pb) lanthanum-zirconate-titanate (PLZT) polarizer and another polarizing filter, PF3, were inserted after BS2. The input voltage to the PLZT polarizer could control the rotation angle of its polarizing axis. The polarizing axis of PF3 was set at the same rotation angle as PF2. When there was no voltage input to the PLZT, only the reference white could pass through PF3. When the axis of the PLZT was rotated by 90 deg, only the test stimuli could pass. In this way the reference white could be substituted for the test stimulus in proportion to the sine of the rotation angle of the PLZT polarizing axis. Either test 1 or test 2 was selected by two electromagnetic shutters, SH1 and SH2, placed in the focal plane of the light beam in each channel. SH3 was used only in experiment 3.

A circular stimulus field of 1.5 deg, 10', or 3.4', made by an aperture AP, was presented at the fovea of the observer's right eye. The surrounding of the stimulus field was dark. The observer's head was fixed by a dental bite board.

Observers

Two males, TT and KU, 26 and 37 years of age, respectively, participated as observers. They had normal color vision as tested by the Farnsworth-Munsell 100-hue test and were experienced in psychophysical experiments.

Stimuli

A temporal double-pulse method was used. As shown in Fig. 2, two test stimuli, test 1 and test 2, were succes-

sively presented with a stimulus-onset asynchrony (SOA). We designate luminances of 500 and 630 nm as components L_g and L_r , respectively. In experiment 1 we exchanged isoluminant chromatic stimuli [Fig. 2(a)]. When the test L_r was larger than the reference L_r with the total luminance $L_g + L_r$ held constant, the stimulus changed in the red direction (Δ red). Similarly, when the test L_r was smaller than the reference L_r , the test stimulus changed in the green direction (Δ green). Four possible combinations of test 1 and test 2 were studied: Δ red + Δ red, Δ green + Δ green, Δ red + Δ green, and Δ green + Δ red. In experiment 2, luminance changes of increment (Δ inc) and decrement (Δ dec) were investigated [Fig. 2(b)]. Again, four combinations of test 1 and test 2 were tested: Δ inc + Δ inc, Δ dec + Δ dec, Δ inc + Δ dec, and Δ dec + Δ inc.

In experiments 1 and 2 the temporal waveform of the test stimulus was a trapezoid shape, as depicted in Fig. 2, because of the large electric capacity of the PLZT polarizer, which caused a slow rising-and-falling temporal response to a rectangular input signal. The SOA was varied from 20 to 2000 ms. The stimulus field subtended a 1.5-deg visual angle. In experiment 3 we used small stimulus fields to examine whether the size of the stimulus field influenced the integration properties obtained in experiments 1 and 2. The field sizes were a 1.5-deg, a 10', and a 3.4' visual angle for the conditions of chromatic exchanges (Δ red + Δ red and Δ red + Δ green). The stimulus durations were 10, 20, and 60 ms, respectively. Since the chromatic exchange could not be observed for short durations when the stimulus field was small, longer

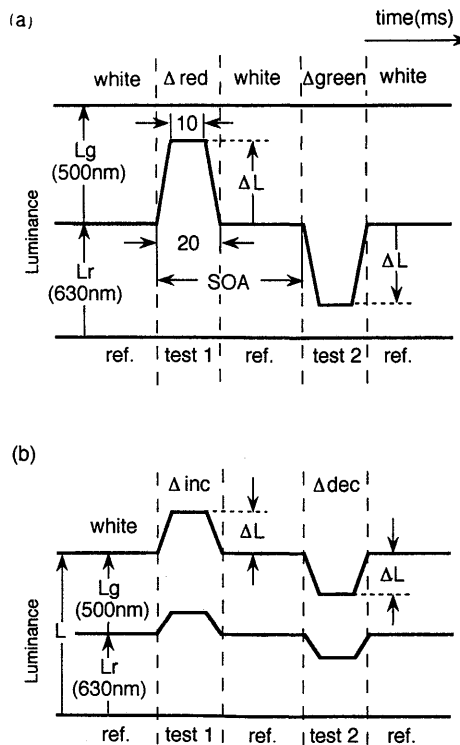


Fig. 2. Temporal stimulus waveform and time course of presenting double-pulse stimuli. (a) Chromatic-exchange condition, (b) luminance-exchange condition. L_g and L_r represent luminances of 500- and 630-nm monochromatic lights. ΔL indicates (a) luminance difference of L_g or L_r between the test and the reference stimuli, (b) luminance difference of $L_g + L_r$ between the test and the reference stimuli.

durations were used for the smaller fields. For the conditions of achromatic exchange ($\Delta \text{inc} + \Delta \text{inc}$), field sizes of 1.5 deg and 3.4' were used, and the stimulus durations were 10 and 30 ms, respectively. We removed the polarizers in order to increase retinal illuminance of the stimuli. Electromagnetic shutters were used to switch between the reference and the test stimuli. The temporal waveform of the stimulus was rectangular. KU was the observer in experiment 3.

The reference white for each observer was set to be neither reddish nor greenish. The retinal illuminance of the reference white was 10 trolands (Td) in experiments 1 and 2 and 30 or 10 Td in experiment 3. The CIE 1931 chromaticity coordinates of the reference white were ($x = 0.375, y = 0.377$) for observer TT and ($x = 0.367, y = 0.379$) for observer KU. White stimuli in tests 1 and 2 were determined by visual color matching to the reference white for each observer. For the chromatic-exchange condition, each observer equated test stimuli 1 and 2 for luminance to the reference white by flicker photometry. For the luminance-exchange condition, only white stimuli in tests 1 and 2 were used.

Procedure

The constant-stimulus method was used to determine detection threshold. In each trial the reference white was presented steadily; then 0.5 s after a buzzer signal, test stimuli 1 and 2 were presented. The observer responded yes when he detected any temporal change in the stimulus field or no if no change was detected.

In the chromatic-exchange condition, the luminance difference ΔL between the test and the reference stimuli, as shown in Fig. 2(a), was taken as a stimulus variable for both Δred and Δgreen pulses. In the luminance-exchange condition, the total luminance difference ΔL , as shown in Fig. 2(b), was used as the stimulus variable. In the preliminary sessions, either test 1 or test 2 was presented so that single-pulse thresholds could be determined. In the main sessions, ΔL 's of tests 1 and 2 increased or decreased in the same ratio relative to those predetermined single-pulse thresholds. The single-pulse thresholds were determined again in the main sessions to obtain those final values for later calculations.

In a session, all conditions of SOA ranging from 20 to 2000 ms and two single-pulse conditions for tests 1 and 2 were chosen at random. The number of conditions in a session was 17 in experiment 1, 18 in experiment 2, and 9–12 in experiment 3. All responses were accumulated as a function of ΔL . The total number of trials was 20–30 when approximately 50% of the responses for ΔL were yes, but fewer trials were run when yes responses for ΔL were near 0 or 100%. A probit analysis was used to obtain the best-fit probability-of-detection curve.¹⁹ We took a 50% detection probability for a threshold value.

Retinal illuminance was raised to 30 Td in the chromatic-exchange condition of experiment 3 so that the observer could detect chromatic change in small stimulus fields. However, at 30 Td the observer noticed a subtle luminance artifact between the test stimulus and the reference white. At this luminance level it was difficult, with the use of electromagnetic shutters, to make perfect substitution with no apparent luminance change, although the luminance artifact was of less than 1-ms duration in

the present apparatus. In experiment 3 the 30-Td retinal illuminance was used only for the chromatic condition, i.e., $\Delta \text{red} + \Delta \text{red}$ and $\Delta \text{red} + \Delta \text{green}$. We used a criterion of change in chromaticity instead of any detectable change in the stimulus field.²⁰

3. RESULTS AND DISCUSSION

We used a summation index to show integration properties between two pulses.²¹ The summation index is defined as

$$\text{summation index} = -\log[(r_1 + r_2)/2],$$

where

$$r_1 = \Delta L (\text{test 1})/\Delta L (\text{test 1, single}),$$

$$r_2 = \Delta L (\text{test 2})/\Delta L (\text{test 2, single}).$$

$\Delta L (\text{test 1})$ and $\Delta L (\text{test 2})$ represent double-pulse threshold; $\Delta L (\text{test 1, single})$ and $\Delta L (\text{test 2, single})$ represent single-pulse threshold. If two pulses were completely integrated, the summation index would be 0.3, as $r_1 = 1/2$, $r_2 = 1/2$. If two pulses were independent and no probability summation took place for two pulses, then $r_1 = 1$ and $r_2 = 1$, and the summation index would be 0.

A. Chromatic Integration (Experiment 1)

Figures 3(a) and 3(b) show the summation index as a function of SOA obtained in the conditions of $\Delta \text{red} + \Delta \text{red}$ and $\Delta \text{green} + \Delta \text{green}$, respectively, for two observers. In both figures, the summation index is ~ 0.3 when

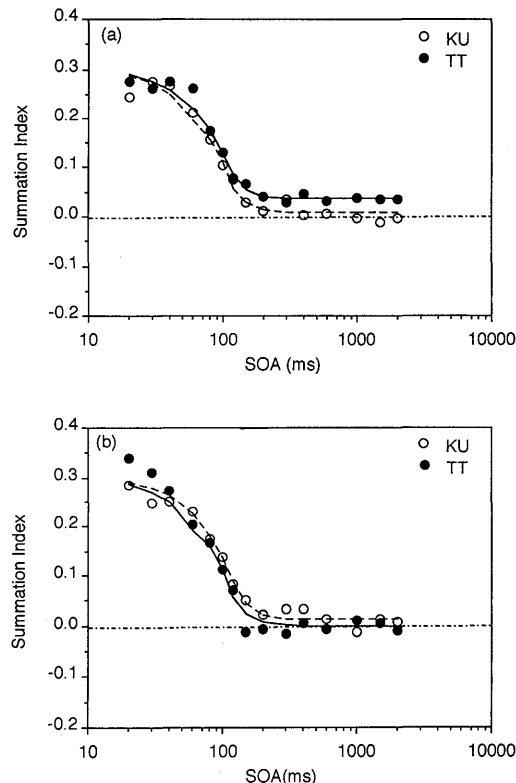


Fig. 3. (a) Summation index as a function of SOA obtained in the conditions of $\Delta \text{red} + \Delta \text{red}$ for two observers. The solid and the dashed curves are the best-fit theoretical functions obtained by a model described in the text. (b) Same as (a) but for $\Delta \text{green} + \Delta \text{green}$.

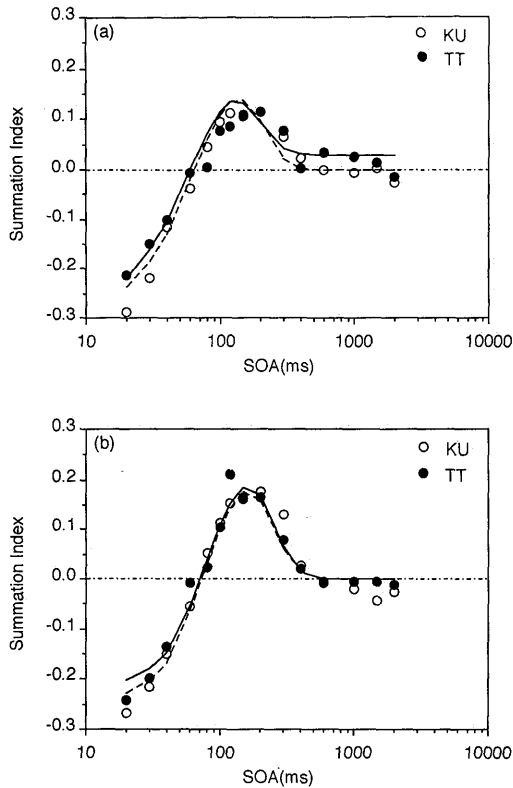


Fig. 4. (a) Same as Fig. 3 but for Δ red + Δ green, (b) same as (a) but for Δ green + Δ red.

the SOA is shorter than 30 ms, indicating that complete summation takes place between two pulses. As the SOA increases to 200 ms, the summation index monotonically decreases, which shows that partial summation occurs and gradually diminishes. The summation index asymptotes for SOA's longer than 200 ms. The Δ red + Δ red and the Δ green + Δ green curves were similar. The solid and the dashed curves drawn along the data points are theoretical functions calculated by using a model, which is described in Subsection 3.E.

Figures 4(a) and 4(b) show the summation-index functions obtained in the conditions of Δ red + Δ green and Δ green + Δ red, respectively. When the SOA is shorter than 60 ms, the summation index has small negative values, indicating that Δ red and Δ green pulses cancel one another. The summation index increases with increasing SOA and has a peak at a SOA of \sim 150 ms and then decreases and asymptotes at a SOA of \sim 500 ms. It is interesting that the summation-index functions peak at a SOA of 150 ms for these conditions.

The summation-index functions obtained for chromatic exchanges of the same direction, Δ red + Δ red and Δ green + Δ green (Fig. 3), are monotonically decreasing functions. This indicates that the chromatic response consists of an excitatory phase. However, the summation-index functions for the opposite chromatic directions, Δ red + Δ green and Δ green + Δ red (Fig. 4), have peaks at a SOA of 150 ms. These peaks cannot be caused by cancellation of an excitatory phase of Δ red with an opposite-polarity excitatory phase of Δ green, since this cancellation would predict a monotonically increasing function. The summation-index functions of Δ red + Δ green and Δ green + Δ red would be explained if the

chromatic response had an inhibitory phase following an excitatory phase, which is contradictory to the results obtained in the Δ red + Δ red and Δ green + Δ green conditions.

B. Achromatic Integration (Experiment 2)

Figures 5(a) and 5(b) show the summation-index functions for the conditions of Δ inc + Δ inc and Δ dec + Δ dec, respectively. The summation index decreases abruptly from 0.3 to a negative value as the SOA increases from 20 to 80 ms. The summation index shows a deep trough at a SOA of 80 ms and then a peak at a SOA of 150 ms. The functions obtained with these Δ inc and Δ dec pulses are similar in shape.

Figures 6(a) and 6(b) show the summation-index functions for the conditions of Δ inc + Δ dec and Δ dec + Δ inc, respectively. The summation index has a negative value at a SOA of 20 ms but increases quickly and reaches a peak at a SOA of 80 ms. When the SOA is longer than 80 ms, the summation index decreases to a constant level.

The summation-index functions for achromatic changes of the same direction, Δ inc + Δ inc and Δ dec + Δ dec (Fig. 5), are not monotonic functions but show a trough and a peak at SOA's of 80 and 150 ms, respectively. It has been shown that the trough of the achromatic summation function indicates an inhibitory phase of the achromatic response.^{16,17} In the conditions of achromatic changes with opposite direction, Δ inc + Δ dec and Δ dec + Δ inc (Fig. 6), the peak of the summation-index functions at a SOA of 80 ms indicates the same inhibitory phase of the achromatic response. However, in Fig. 6 there is no trough that corresponds to the peak at a SOA of 150 ms in the functions shown in Fig. 5. This is another contradic-

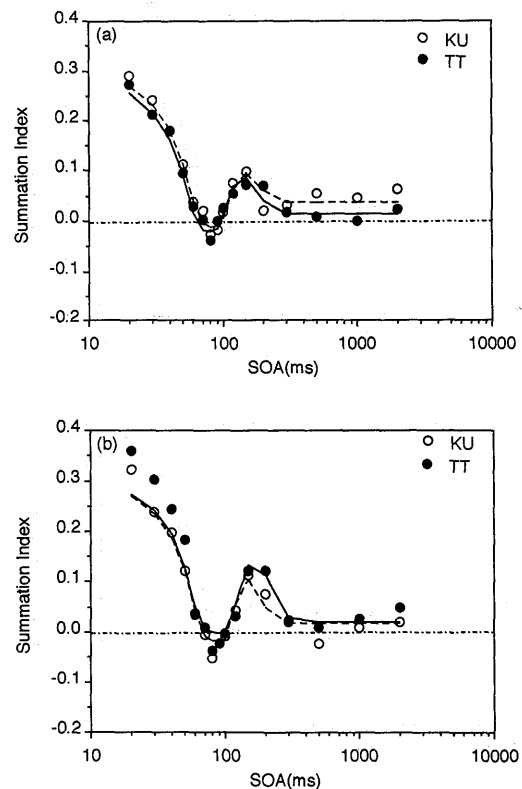


Fig. 5. (a) Same as Fig. 3 but for Δ inc + Δ inc, (b) same as (a) but for Δ dec + Δ dec.

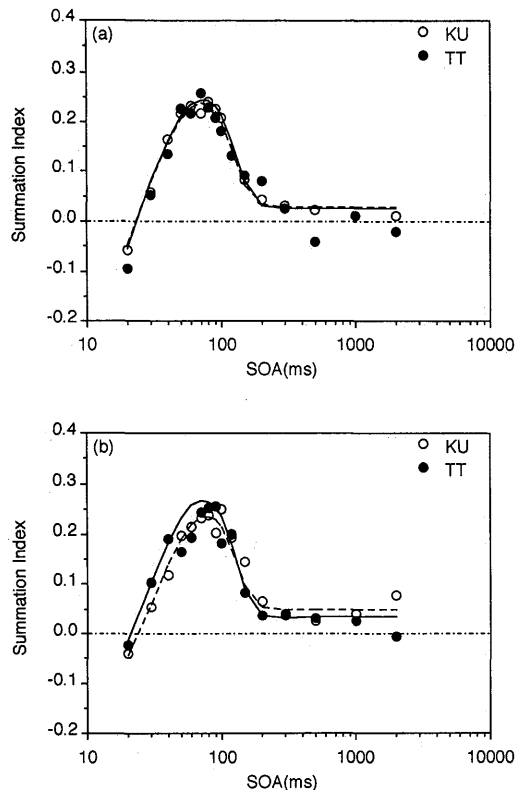


Fig. 6. (a) Same as Fig. 3 but for Δ inc + Δ dec, (b) same as (a) but for Δ dec + Δ inc.

tion between the results obtained for stimuli that change in the same direction and for those that change in the opposite direction.

C. Small Fields (Experiment 3)

Figures 7(a), 7(b), and 7(c) show the summation-index functions with stimulus fields of 1.5 deg, 10', and 3.4', respectively, for the conditions of Δ red + Δ red and Δ red + Δ green. The summation-index functions with 10' and 3.4' fields are the same as those with 1.5-deg fields for the conditions of both Δ red + Δ red and Δ red + Δ green. The peaks of the Δ red + Δ green function at a SOA of ~100–150 ms still appear for small fields.

Figures 8(a) and 8(b) show the summation-index functions with stimulus fields of 1.5 deg and 3.4', respectively, for the condition of Δ inc + Δ inc. The summation-index function for the 3.4' stimulus field does not have a dip at a SOA of 80 ms, but it is a fairly smooth decreasing function. These effects of small stimulus fields on luminance response have been obtained in previous investigations.²²

We show in these experiments that small stimulus fields do not affect the shape of the summation-index functions of chromatic changes. On the contrary, small stimulus fields affect achromatic integration. As shown in Fig. 8, the trough of the Δ inc + Δ inc function almost disappeared with the 3.4' field. It seems likely that the inhibitory phase at a SOA of 80 ms becomes smaller for the stimulus field of 3.4'.

D. Implications of Chromatic and Achromatic Summation-Index Functions

It has been indicated that the chromatic response has a slow excitation phase, which can be inferred from the

chromatic modulation transfer function with low-pass filter characteristics.⁶ In the present experiments we confirmed this monophasic chromatic response with the conditions of Δ red + Δ red and Δ green + Δ green. However, we obtained contradictory results in the Δ red + Δ green and Δ green + Δ red conditions. These results suggested that the chromatic response was biphasic, consisting of both excitatory and inhibitory phases, which to our knowledge has not been pointed out in previous research.

When we carefully examined the results of achromatic changes, we found the same contradictory results. For the Δ inc + Δ inc and the Δ dec + Δ dec conditions (see Fig. 5), the peak of the summation-index function at a SOA of 150 ms indicates a small excitatory phase, which follows an inhibitory phase, of the achromatic response. The response function consists of three phases: the first, excitatory phase; the second, inhibitory phase; and the third, excitatory phase. However, in the Δ inc + Δ dec and the Δ dec + Δ inc conditions (see Fig. 6), there was no trough,

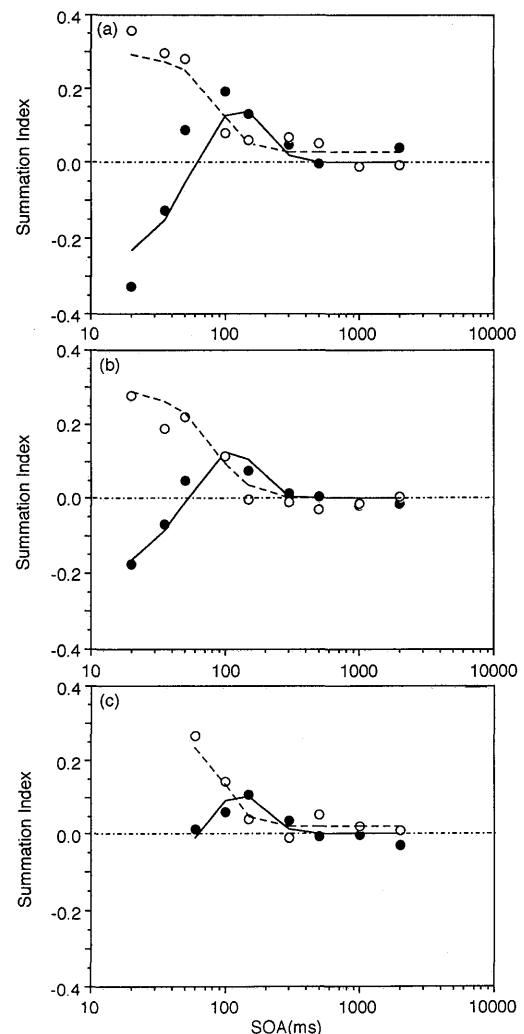


Fig. 7. (a) Summation index as a function of a SOA obtained in the conditions of Δ red + Δ red (open circles) and Δ red + Δ green (filled circles) for a stimulus field of 1.5 deg and a duration of 10 ms for observer KU. The solid and the dashed curves are the best-fit theoretical functions obtained by a model described in the text. (b) Same as (a) but for a stimulus field of 10' and a duration of 20 ms, (c) same as (a) but for a stimulus field of 3.4' and a duration of 60 ms.

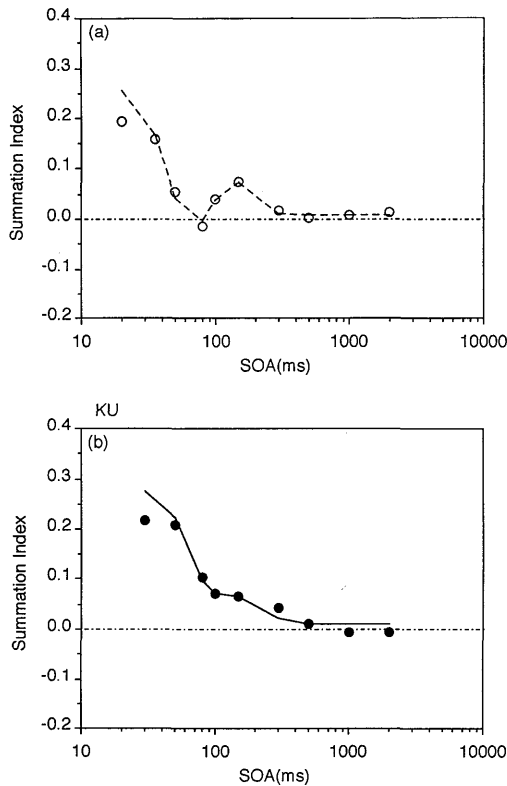


Fig. 8. (a) Summation index as a function of a SOA obtained in the conditions of $\Delta \text{inc} + \Delta \text{inc}$ (open circles) for a stimulus field of 1.5 deg and a duration of 10 ms for observer KU. The curve is the best-fit theoretical function obtained by a model described in the text. (b) Same as (a) but for a stimulus field of 3.4' and a duration of 30 ms.

which should correspond to the third, excitatory phase, in the summation-index functions. A triphasic response function of achromatic changes also was suggested by Roufs and Blommaert.¹⁸ Our results for $\Delta \text{inc} + \Delta \text{inc}$ and $\Delta \text{dec} + \Delta \text{dec}$ support the triphasic function, whereas those for $\Delta \text{inc} + \Delta \text{dec}$ and $\Delta \text{dec} + \Delta \text{inc}$ indicate the biphasic function.

When we compare the chromatic and the achromatic summation-index functions, we notice that the chromatic functions of $\Delta \text{red} + \Delta \text{red}$ and $\Delta \text{green} + \Delta \text{green}$ (see Fig. 3) are different from the achromatic functions of $\Delta \text{inc} + \Delta \text{inc}$ and $\Delta \text{dec} + \Delta \text{dec}$ (see Fig. 5) at SOA's of 80 and 150 ms, where the achromatic functions have a trough and a peak. On the other hand, they are similar in that they reach constant levels at SOA's that are longer than 200–300 ms. Furthermore, the peaks of the chromatic functions of $\Delta \text{red} + \Delta \text{green}$ and $\Delta \text{green} + \Delta \text{red}$ (see Fig. 4) at a SOA of 150 ms correspond to the peaks of the achromatic functions of $\Delta \text{inc} + \Delta \text{inc}$ and $\Delta \text{dec} + \Delta \text{dec}$ (see Fig. 5). These differences and similarities in chromatic and achromatic functions seem to suggest that it would be possible to describe chromatic and achromatic responses by using common excitatory and inhibitory phases. These phases are subtracted for the achromatic response and are added for the chromatic response with some temporal delay. A similar description of chromatic and luminance responses was used by Burbeck and Kelly¹² and by Kelly¹³ to explain chromatic and luminance modulation transfer functions. Moreover, the possible inhibi-

tory phase of the chromatic response and the third, excitatory phase of the achromatic response might be explained by a common mechanism.

Figures 7 and 8 show that the chromatic summation-index functions for the small fields, 10' and 3.4', are almost the same as those for the large field, 1.5 deg, but that the achromatic function for the small field is quite different from that for the large field. These results indicate that the inhibitory phase of chromatic response at a SOA of 150 ms does not change with decreasing stimulus size, whereas the inhibitory phase of the achromatic response at a SOA of 80 ms becomes smaller. This means that the achromatic and the chromatic inhibitory phases originate from different levels of the visual system. The former might be a result of spatial antagonistic organization of the opponent receptive field, in which excitatory and inhibitory properties should depend on the size of the stimulus. The latter might be from higher visual mechanisms, which would lose this kind of spatial organization.

Some kind of asymmetrical mechanism is needed to explain the biphasic chromatic response and the triphasic achromatic response. These responses were obtained only with double pulses of opposite polarities, which implies that a potential response somehow remains after termination of a stimulus. This potential response is effective only with the opposite-polarity stimulus. We postulate a rebound phase from a preceding negative phase as this asymmetrical mechanism, which is described in detail in Subsection 3.E.

E. Derivation of Impulse-Response Functions

We tried using a unitary model to derive impulse-response functions for describing our data. If a unitary model can explain the present data, it is theoretically possible to make a parallel model that explains all the data. The parallel model can have the same properties as the unitary model, because a parallel model has more free parameters than does a unitary model. Thus it would be meaningful to see whether a unitary model, which has more restrictions than does a parallel model, would work on the present data. Our model, depicted in Fig. 9, consists of three levels. Level I corresponds to the L and the M cones, and level II corresponds to the L-M and the M-L opponent mechanisms. It seems plausible to postulate that level I is connected to level II by excitatory transformation (solid line) and inhibitory transformation (dashed line). The

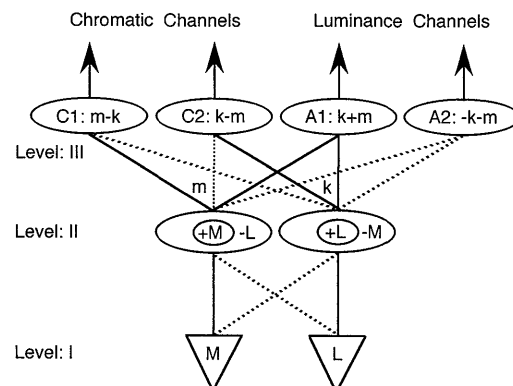


Fig. 9. Three-level model used to derive the impulse response functions of chromatic and achromatic changes.

Table 1. Parameters of Impulse Response Functions Derived to Give Best Fit to the Chromatic and the Achromatic Summation-Index Functions^a

	H1			H2				H3				
	A	τ (ms)	n	A	τ (ms)	n	t_{d1} (ms)	A	τ (ms)	n	t_{d2} (ms)	β
Observer KU												
Experiment 1												
$\Delta r + \Delta r$; Δr	1	35	3	0.90	25	3	75	—	—	—	—	33
$\Delta g + \Delta g$; Δg	1	35	3	0.90	30	3	65	—	—	—	—	23
$\Delta r + \Delta g$; Δr	-1	35	3	-0.72	25	3	75	0.95	40	3	155	—
$\Delta g + \Delta r$; Δg	1	35	3	0.72	25	3	75	—	—	—	—	inf.
$\Delta g + \Delta r$; Δg	-1	35	3	-0.97	25	3	75	1.55	40	4	150	—
$\Delta r + \Delta g$; Δr	1	35	3	0.97	25	3	75	—	—	—	—	inf.
Experiment 2												
$\Delta i + \Delta i$; Δi	1	35	3	-0.92	20	3	75	0.17	20	3	150	8
$\Delta d + \Delta d$; Δd	1	35	3	-1.00	20	3	75	0.20	20	3	160	18
$\Delta i + \Delta d$; Δi	-1	35	3	1.00	25	3	70	—	—	—	—	—
$\Delta d + \Delta i$; Δd	1	35	3	-1.00	25	3	70	0.70	25	4	150	10
$\Delta d + \Delta i$; Δd	-1	35	3	1.03	25	3	75	—	—	—	—	—
$\Delta i + \Delta d$; Δi	1	35	3	-1.03	25	3	75	0.63	20	4	150	6
Experiment 3												
1.5 deg												
$\Delta r + \Delta r$; Δr	1	35	3	0.2	20	3	60	—	—	—	—	10
$\Delta r + \Delta g$; Δr	-1	35	3	-0.45	20	3	75	0.89	40	3	140	—
$\Delta g + \Delta r$; Δg	1	35	3	0.45	20	3	75	—	—	—	—	inf.
$\Delta i + \Delta i$; Δi	1	35	3	-1.00	20	3	60	0.15	20	3	120	30
10'												
$\Delta r + \Delta r$; Δr	1	35	3	0.2	20	3	60	—	—	—	—	inf.
$\Delta r + \Delta g$; Δr	-1	35	3	-0.45	25	3	65	0.68	30	3	140	—
$\Delta g + \Delta r$; Δg	1	35	3	0.45	25	3	65	—	—	—	—	inf.
3.4'												
$\Delta r + \Delta r$; Δr	1	35	3	0.2	20	3	60	—	—	—	—	15
$\Delta r + \Delta g$; Δr	-1	35	3	-1.17	25	3	75	1.08	30	3	140	—
$\Delta g + \Delta r$; Δg	1	35	3	1.17	25	3	75	—	—	—	—	inf.
$\Delta i + \Delta i$; Δi	1	35	3	-0.18	20	3	90	0.10	40	3	180	25
Observer TT												
Experiment 1												
$\Delta r + \Delta r$; Δr	1	35	3	0.90	25	3	65	—	—	—	—	8
$\Delta g + \Delta g$; Δg	1	35	3	0.80	25	3	75	—	—	—	—	inf.
$\Delta r + \Delta g$; Δr	-1	35	3	-1.00	25	3	75	1.13	40	3	150	—
$\Delta g + \Delta r$; Δg	1	35	3	1.00	25	3	75	—	—	—	—	10
$\Delta g + \Delta r$; Δg	-1	35	3	-0.83	25	3	75	1.50	40	4	150	—
$\Delta r + \Delta g$; Δr	1	35	3	0.83	25	3	75	—	—	—	—	inf.
Experiment 2												
$\Delta i + \Delta i$; Δi	1	35	3	-0.82	15	3	75	0.11	25	3	160	20
$\Delta d + \Delta d$; Δd	1	35	3	-0.90	20	3	75	0.30	30	3	160	15
$\Delta i + \Delta d$; Δi	-1	35	3	1.00	25	3	75	—	—	—	—	—
$\Delta d + \Delta i$; Δd	1	35	3	-1.00	25	3	75	0.63	25	4	150	11
$\Delta d + \Delta i$; Δd	-1	35	3	1.17	25	3	75	—	—	—	—	—
$\Delta i + \Delta d$; Δi	1	35	3	-1.17	25	3	75	0.65	20	3	150	9

^a $\Delta r, \Delta$ red; $\Delta g, \Delta$ green; $\Delta i, \Delta$ inc; $\Delta d, \Delta$ dec; inf., infinity

model assumes that the inhibitory response between levels I and II has a certain temporal delay relative to the excitatory response. Kelly² and Ingling and Martinez¹⁴ proposed similar mechanisms. In level III there are four possible combinations of addition (excitatory connection) and subtraction (inhibitory connection) of the L-M and the M-L opponent responses.

In order to give quantitative values to the model, we obtained the summation-index functions best fitted to the

data points by using a low-pass-filter model. An n -stage low-pass filter is expressed by

$$H(t) = A/\tau(t/\tau)^{n-1} \exp[-(t/\tau)] / (n-1)!,$$

where A is a proportional constant and τ is a time constant.⁴ Let $H1(t)$ be the excitatory phase and $H2(t - t_{d1})$ be the inhibitory phase, both of which come from level I. A t_{d1} represents a temporal delay of the inhibitory phase

relative to the excitatory phase. $H1(t)$ and $H2(t - t_{d1})$ are summed in level II.

When an isoluminant chromatic stimulus Δ red is presented to level I, $H1(t)$ of the L cone changes in a positive direction, but $H1(t)$ of the M cone changes in a negative direction. This is because the red luminance component L_r of Δ red is greater than the luminance component of the reference white, whereas the green luminance component L_g is smaller (see Fig. 2). $H2(t - t_{d1})$ of the L cone becomes negative, and $H2(t - t_{d1})$ of the M cone becomes positive, with inhibitory connections between the L and M cones and the L-M and M-L mechanisms. Thus the L-M mechanism receives, first, $H1(t)$ from the L cone and then, with a temporal delay t_{d1} , $H2(t - t_{d1})$ from the M cone, yielding an output $k = H1(t) + H2(t - t_{d1})$, a positive monophasic response. Similarly, the M-L mechanism produces $m = H1(t) + H2(t - t_{d1})$, a negative monophasic response. When a luminance increment stimulus Δ inc is presented to level I, $H1(t)$'s of the L and the M cones change in the positive direction and $H2(t - t_{d1})$'s change in the negative direction. $k, m = H1(t) + H2(t - t_{d1})$ of the L-M and the M-L mechanisms are the same biphasic responses.

We made an assumption in order to account for the contradictory results shown in experiments 1 and 2. When either the k response or the m response terminates while in a negative phase, a positive rebound phase, $H3(t - t_{d2})$, should be added following the negative phase, with a temporal delay t_{d2} in level III; but no negative rebound phase occurs following a final positive phase. Thus the final impulse response $HF(t)$ coming out of level III is defined as follows:

$$C1: HF(t) = m - k + H3(t - t_{d2}),$$

$$C2: HF(t) = k - m + H3(t - t_{d2}),$$

$$A1: HF(t) = k + m + H3(t - t_{d2}),$$

$$A2: HF(t) = -k - m + H3(t - t_{d2}).$$

When a Δ red is presented, for example, the m response consists of a negative phase and the k response consists of a positive phase. Therefore a positive rebound phase, $H3(t - t_{d2})$, is added only to the m response in C1. Then, if a Δ green is presented with a certain SOA, the m response becomes a positive phase, which is summed with the positive rebound phase of the first Δ red in level III. As a result, $HF(t)$ of C1 becomes a large positive response at this SOA. If the second pulse is a Δ red, the m response is negative, which cancels the positive rebound of the first Δ red at the same SOA, and C1 yields no large response. Similarly, C2 makes a large positive response at the same SOA when the first and the second pulses are Δ green and Δ red, respectively.

In the case of luminance pulses, when a Δ inc is presented, the k response and the m response are the same biphasic responses, the first being positive phase and the second being negative phase. Therefore $H3(t - t_{d2})$ is added to both the k response and the m response in A1. $H3(t - t_{d2})$ of Δ inc affects only the second Δ inc but is canceled by the response of the second Δ dec. When the first pulse is Δ dec, A2 plays the same role as A1.

The total response $R(t)$ caused by the input pulse $I(t)$ is determined by the convolution integral

$$R(t) = \int_0^t I(t')HF(t - t')dt'.$$

We adopted the temporal probability-summation model of Watson²³ as our detection-threshold mechanism. The detection probability, P , is defined by

$$P = 1 - \exp \left[- \int_0^T |R(t)|^\beta dt \right],$$

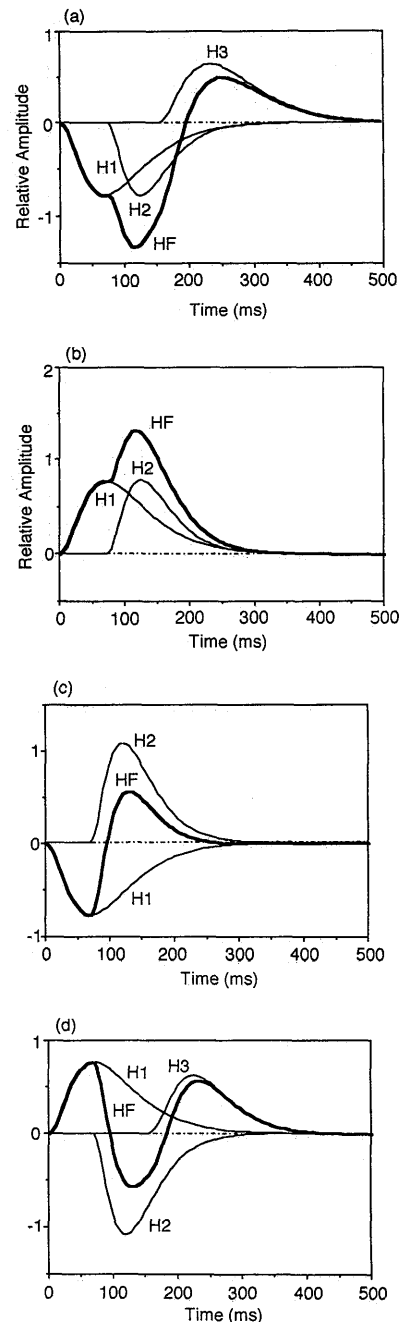


Fig. 10. Impulse response function HF (thick curves) of (a) C1 mechanism for Δ red, (b) C1 mechanism for Δ green, (c) A2 mechanism for Δ inc, (d) A2 mechanism for Δ dec. Thin curves represent component responses. Observer: KU.

where β is the empirical parameter and T is chosen large enough that $R(T)$ is equal to 0. This equation has been shown to be a general form of the temporal summation.²³ It becomes the peak-or-trough detector model and the power-integrator model when β is set equal to infinity and to 2, respectively.

The parameters A , τ , n , t_{d1} , t_{d2} , and β were determined by the least-squares method so that the best-fit summation-index values were obtained. The solid and the dashed curves shown in Figs. 3–8 were obtained by this fitting procedure. Table 1 shows each parameter for the curves in Figs. 3–8. It should be noticed that $H1$ in all figures have the same shape. The fit is quite good for all experimental conditions. The $HF(t)$'s of C1 obtained for Δ red and Δ green are shown in Figs. 10(a) and 10(b), respectively. The $HF(t)$ functions are shown by thick curves. The thin curves represent the component responses $H1(t)$, $H2(t - t_{d1})$, and $H3(t - t_{d2})$. The $HF(t)$'s of A2 obtained for Δ inc and Δ dec are shown in Figs. 10(c) and 10(d), respectively.

Increasing numbers of reports suggest that the cells of the magnocellular pathway form the physiological substrate for the detection of luminance modulation and that the cells of the parvocellular pathway form the substrate for detection of chromatic modulation.^{8–10} These findings support a parallel model. The temporal delay between the excitatory and the inhibitory phases turned out to be ~ 75 ms for most of the cases. Although this value is consistent with those of previous studies,^{6,16,17,22,24} a physiological study showed that the center-surround delay of a macaque ganglion receptive field was 3–8 ms.¹⁰ It should be noted that we did not attempt to build a complete physiological model with our data but tried to devise a model that could generate chromatic and achromatic impulse response functions that gave the summation-index functions best fitted to our data.

ACKNOWLEDGMENT

We thank P. K. Kaiser for his critical comments and his help in preparing the manuscript.

REFERENCES AND NOTES

1. D. H. Kelly and D. van Norren, "Two-band model of heterochromatic flicker," *J. Opt. Soc. Am.* **67**, 1081–1091 (1977).
2. D. H. Kelly, "Spatial and temporal interactions in color vision," *J. Imag. Tech.* **15**, 82–89 (1989).
3. V. C. Smith, R. W. Bowen, and J. Pokorny, "Threshold temporal integration of chromatic stimuli," *Vision Res.* **24**, 653–660 (1984).
4. K. Uchikawa and M. Ikeda, "Temporal integration of chromatic double pulses for detection of equal-luminance wavelength changes," *J. Opt. Soc. Am. A* **3**, 2109–2115 (1986).

5. K. Uchikawa, "Temporal integration for wavelength change of an equal-luminance single pulse," *J. Light Vis. Environ.* **13**, 69–75 (1989).
6. W. H. Swanson, T. Ueno, V. C. Smith, and J. Pokorny, "Temporal modulation sensitivity and pulse-detection thresholds for chromatic and luminance perturbations," *J. Opt. Soc. Am. A* **4**, 1992–2005 (1987).
7. S. L. Guth, R. W. Massof, and T. Benzschawel, "Vector model for normal and dichromatic vision," *J. Opt. Soc. Am.* **70**, 197–212 (1980).
8. C. R. Ingling, Jr., and B. H.-P. Tsou, "Orthogonal combination of the three visual channels," *Vision Res.* **17**, 1075–1082 (1977).
9. B. B. Lee, P. R. Martin, and A. Valberg, "Sensitivity of macaque ganglion cells to luminance and chromatic flicker," *J. Physiol.* **414**, 223–243 (1989).
10. B. B. Lee, P. R. Martin, and A. Valberg, "Amplitude and phase of responses of macaque retinal ganglion cells to flickering stimuli," *J. Physiol.* **414**, 245–263 (1989).
11. B. B. Lee, J. Pokorny, V. C. Smith, P. R. Martin, and A. Valberg, "Luminance and chromatic modulation sensitivity of macaque ganglion cells and human observers," *J. Opt. Soc. Am. A* **7**, 2223–2236 (1990).
12. C. A. Burbeck and D. H. Kelly, "Spatiotemporal characteristics of visual mechanisms: excitatory-inhibitory model," *J. Opt. Soc. Am.* **70**, 1121–1126 (1980).
13. D. H. Kelly, "Spatiotemporal variation of chromatic and achromatic constant thresholds," *J. Opt. Soc. Am.* **73**, 742–750 (1983).
14. C. R. Ingling, Jr., and E. Martinez-Uriegas, "The spatiotemporal properties of the r-g X-cell channel," *Vision Res.* **25**, 33–38 (1985).
15. P. Gouras and E. Zrenner, "Enhancement of luminance flicker by color-opponent mechanisms," *Science* **205**, 587–589 (1979).
16. M. Ikeda, "Temporal summation of positive and negative flashes in the visual system," *J. Opt. Soc. Am.* **55**, 1527–1534 (1965).
17. J. A. J. Roufs, "Dynamic properties of vision—III. Twin flashes, single flashes and flicker fusion," *Vision Res.* **13**, 309–323 (1973).
18. J. A. J. Roufs and F. J. J. Blommaert, "Temporal impulse and step responses of the human eye obtained psychophysically by means of a drift-correcting perturbation technique," *Vision Res.* **21**, 1203–1221 (1981).
19. D. J. Finney, *Probit Analysis*, 3rd ed. (Cambridge U. Press, Cambridge, 1971).
20. By this criterion, the observer responded only to changes in chromaticity in the stimulus field and ignored other changes, if any. The effectiveness of this criterion for isolating chromatic pathways has been shown by J. J. Wisowaty, "Estimates for the temporal response characteristics of chromatic pathways," *J. Opt. Soc. Am.* **71**, 970–977 (1981), and in Ref. 4.
21. R. M. Boynton, M. Ikeda, and W. S. Stiles, "Interactions among chromatic mechanisms as inferred from positive and negative increment thresholds," *Vision Res.* **4**, 87–117 (1964).
22. J. G. Meijer, G. J. van der Wildt, and G. van den Brink, "Twin-flash response as a function of flash diameter," *Vision Res.* **18**, 1111–1116 (1978).
23. A. B. Watson, "Probability summation over time," *Vision Res.* **19**, 515–522 (1979).
24. A. B. Watson and J. Nachmias, "Patterns of temporal interaction in the detection of gratings," *Vision Res.* **17**, 893–902 (1977).